

International Validation of Echocardiographic AI Amyloid Detection Algorithm

Grant Duffy, BS¹, Evan Oikonomou, MD, DPhil², Jonathan Hourmozdi, MD³, Hiroki Usuku, MD, PhD⁴, Jigesh Patel, MD¹, Lily Stern, MD¹, Shinichi Goto, MD, PhD^{5,6}, Kenichi Tsujita, MD, PhD⁴, Rohan Khera, MD, MS², Faraz S. Ahmad, MD³, David Ouyang, MD¹

1. Smidt Heart Institute, Cedars-Sinai Medical Center, Los Angeles, CA, USA
2. Department of Medicine, Yale School of Medicine, New Haven, CT, USA
3. Department of Medicine, Northwestern Medicine, Chicago, IL, USA
4. Department of Cardiovascular Medicine, Graduate School of Medical Sciences, Kumamoto University, Chuo-ku, Kumamoto, Japan
5. One Brave Idea, Brigham and Women's Hospital, Boston, MA, USA
6. Department of Cardiology, Keio University School of Medicine, Shinjuku, Tokyo, Japan.

Correspondence:

David Ouyang, MD
127 S. San Vicente Blvd., Suite A3600
Los Angeles, CA 90048
david.ouyang@cshs.org

Short title: EchoNet-LVH Validation

Word count: [follow target journal guidance]

ABSTRACT

Background

Diagnosis of cardiac amyloidosis (CA) is often missed or delayed due to confusion with other causes of increased left ventricular wall thickness. Conventional transthoracic echocardiographic measurements like global longitudinal strain (GLS) has shown promise in distinguishing CA, but with limited specificity. We conducted a study to investigate the performance of a computer vision detection algorithm in across multiple international sites.

Methods

EchoNet-LVH is a computer vision deep learning algorithm for the detection of cardiac amyloidosis based on parasternal long axis and apical-4-chamber view videos. We conducted a multi-site retrospective case-control study evaluating EchoNet-LVH's ability to distinguish between the echocardiogram studies of CA patients and controls. We reported discrimination performance with area under the receiver operating characteristic curve (AUC) and associated sensitivity, specificity, and positive predictive value at the pre-specified threshold.

Results

EchoNet-LVH had an AUC of 0.896 (95% CI 0.875 – 0.916). At pre-specified model threshold, EchoNet-LVH had a sensitivity of 0.644 (95% CI 0.601 – 0.685), specificity of 0.988 (0.978 – 0.994), positive predictive value of 0.968 (95% CI 0.944 – 0.984), and negative predictive value of 0.828 (95% CI 0.804 – 0.850). There was minimal heterogeneity in performance by site, race, sex, age, BMI, CA subtype, or ultrasound manufacturer.

Conclusion

EchoNet-LVH can assist with earlier and accurate diagnosis of CA. As CA is a rare disease, EchoNet-LVH is highly specific in order to maximize positive predictive value. Further work will assess whether early diagnosis results in earlier initiation of treatment in this underserved population.

INTRODUCTION

Cardiac amyloidosis (CA) is caused by deposition of misfolded proteins in the myocardium, including transthyretin (ATTR) or immunoglobulin light chains (AL). Regardless of the etiology, CA leads to increased left ventricular wall thickness and heart failure, however early symptoms can be non-specific and not readily recognized. Common echocardiographic measurements are insufficient to precisely discriminate CA from other etiologies of left ventricular hypertrophy (LVH) or heart failure.

There is concern that CA is underdiagnosed and diagnosed too late³⁻⁵, which limit the opportunity to receive recent targeted therapies that improve quality of life and decrease mortality outcomes in CA patients^{6,7}. Recent research has focused on methods that can assist with early identification of CA. Echocardiography is one of the most common initial tests when evaluating patients with heart failure symptoms, with typical CA features on including increased left ventricular wall thickness, normal or small left ventricular cavity, preserved left ventricular ejection fraction (LVEF), and diastolic dysfunction¹⁰. However, many of these features are also commonly found in other forms of heart failure with preserved ejection fraction^{11,13}. Individually, these measurements have limiting ability to specifically identify CA, resulting in imaging cardiologists to hesitate to highlight suspicion for CA.

Recent advances in computer vision and artificial intelligence (AI) have enabled precision phenotyping of structure and function in cardiac ultrasound. AI applied to echocardiography can precisely estimate wall thickness²⁰, assess mitral regurgitation severity, and left ventricular ejection fraction (LVEF) as well as detect cardiac amyloidosis, HCM, and diastolic dysfunction. However, many algorithms have not been rigorously validated in multiple centers or undergone prospective evaluation of performance. As such, significant work is needed to evaluate the true performance at individual sites.

In this study, we evaluated the performance EchoNet-LVH, a previously developed a computer vision deep learning algorithm for the detection of cardiac amyloidosis, across multiple new healthcare systems and videos that the model has never seen before. We conducted a multi-site international retrospective case-control study evaluating EchoNet-LVH's ability to distinguish between the echocardiogram studies of CA patients and controls. We reported discrimination performance with area under the receiver operating characteristic curve (AUC) and associated sensitivity, specificity, and positive predictive value at a pre-specified threshold to raise suspicion for CA.

METHODS

Study Design

We conducted an international multicenter retrospective case-control cohort study with participants from multiple geographically distinct healthcare systems to evaluate EchoNet-LVH. EchoNet-LVH was previously developed using CA cases and controls from Stanford Healthcare²⁰, so this study serves as temporally and geographically distinct external validation. Patients were sourced from Cedars-Sinai Medical Center in Los Angeles, California, Keio University in Tokyo, Japan, Northwestern Medicine in Chicago, Illinois, and Yale-New Haven Hospital in New Haven, Connecticut. A total of 520 patients were identified as having CA and matched to 903 randomly selected controls from patients receiving echocardiography and at least 65 years of age. CA patients were diagnosed with transthyretin (ATTR), light chain (AL) amyloidosis, or other forms of cardiac amyloidosis using a combination of pyrophosphate scintigraphy, monoclonal gammopathy testing, genetic testing, and/or tissue biopsy. The controls either had negative testing for cardiac amyloidosis or testing was not performed. Given the low population prevalence of CA, the likelihood of undiagnosed CA in the controls was thought to be minor and unlikely to change the analysis. This study was approved by the Cedars-Sinai Institutional Review Board.

Computer Vision Model

EchoNet-LVH's development approach and internal validation has been previously described²⁰. In short, EchoNet-LVH is an automated machine learning pipeline that automatically identifies parasternal long axis and apical-4-chamber views from transthoracic echocardiogram studies, precisely measures wall thickness, and assesses texture and motion from the apical-4-chamber view echocardiogram videos to assess suspicion for cardiac amyloidosis. Information from the apical-4-chamber view is synthesized with a segmentation model's assessment of wall thickness from the parasternal long axis videos to come up with a suspicion for CA. Given the low population prevalence of CA, a prespecified threshold (0.8) in the summative assessment was chosen to optimize and prioritize for specificity, which in turn, maximizes positive predictive value. Echocardiogram videos were obtained in DICOM format and a fully automatic pipeline analyses the study.

Statistical Analysis

Continuous variables were reported using median (interquartile range), and categorical variables were reported with number (percentage). Performance of TTE measurements, GLS measurements, and ratios in discriminating CA was evaluated using area under the receiver operator curve (AUC). Ninety-five percent confidence intervals were assessed for all analyses. Statistical analysis was performed in Python (Python Software Foundation, Beaverton, Oregon).

RESULTS

Demographics and clinical characteristics of the study cohort are shown in **Table 1**. The mean age of the cohort was 78.2 (IQR 72 – 84) and 77.7% male. In the cases, there was representation from both AL (22.7%) and ATTR (74.2%) amyloidosis. There was a wide range of age, BMI, and ultrasound manufacturers across the sites.

EchoNet-LVH had an overall AUC of 0.896 (95% CI 0.875 - 0.916) with minimal site level variation in performance (**Table 2**). The lowest site AUC was YNHH with an AUC 0.860 (95% CI 0.818 – 0.898) and the highest site AUC was Keio University with an AUC of 0.944 (95% CI 0.911 – 0.971). The overall sensitivity was 0.644 (95% CI 0.601 – 0.685) and the overall specificity was 0.988 (95% CI 0.978 – 0.994). There was no significant heterogeneity in other performance characteristics across site. At a 2:1 ratio of controls to cases, EchoNet-LVH had a PPV of 0.968 (95% CI 0.944 – 0.984) and a NPV of 0.828 (95% CI 0.804 – 0.850).

EchoNet-LVH also had similar performance across patient characteristics and ultrasound manufacturer (**Table 3**). EchoNet-LVH had an AUC of 0.921 (95% CI 0.882 - 0.955) for detecting AL cardiac amyloidosis and an AUC of 0.887 (95% CI 0.862 - 0.911) for detecting ATTR cardiac amyloidosis. Our model had similar performance for men (AUC of 0.893 [95% CI 0.869 – 0.914]) and women (AUC of 0.904 [95% CI 0.849 – 0.950]). There was no significant heterogeneity by race, age, BMI, or ultrasound manufacturer. Across all key groups, there was similar sensitivity and specificity of our approach, and there was no trend for differences in performance across subclasses.

DISCUSSION

In this study, we evaluated the performance of a computer vision driven AI workflow for the detection and screening of cardiac amyloidosis across a wide range of patients from an international cohort of geographically distinct healthcare systems. In this setting, we found EchoNet-LVH had strong performance in identifying patients with CA of all subtypes, and its performance was consistent across sites, ultrasound manufacturers, and patient characteristics.

A few things are worth considering in evaluating our algorithm. Because increased wall thickness is a hallmark of CA²², our algorithm automated the approach to precisely measuring wall thickness as well as integrated this precise measurement with more 'black box' features of motion and texture assessed in the apical-4-chamber view. Our approach homes to minimize or exclude confounders²³, as our models were trained on controls matched on wall-thickness and limit the potential of AI models to shortcut on wall thickness alone. Second, our approach sought to maximize positive predictive value in the downstream testing of CA²⁴. In a rare disease, PPV is significantly impacted by model specificity (as the number of false positives are likely to outweigh the number of potential true positives). We sought to find a balance of sensitivity and specificity as to minimize the number of false positives rejected in downstream testing.

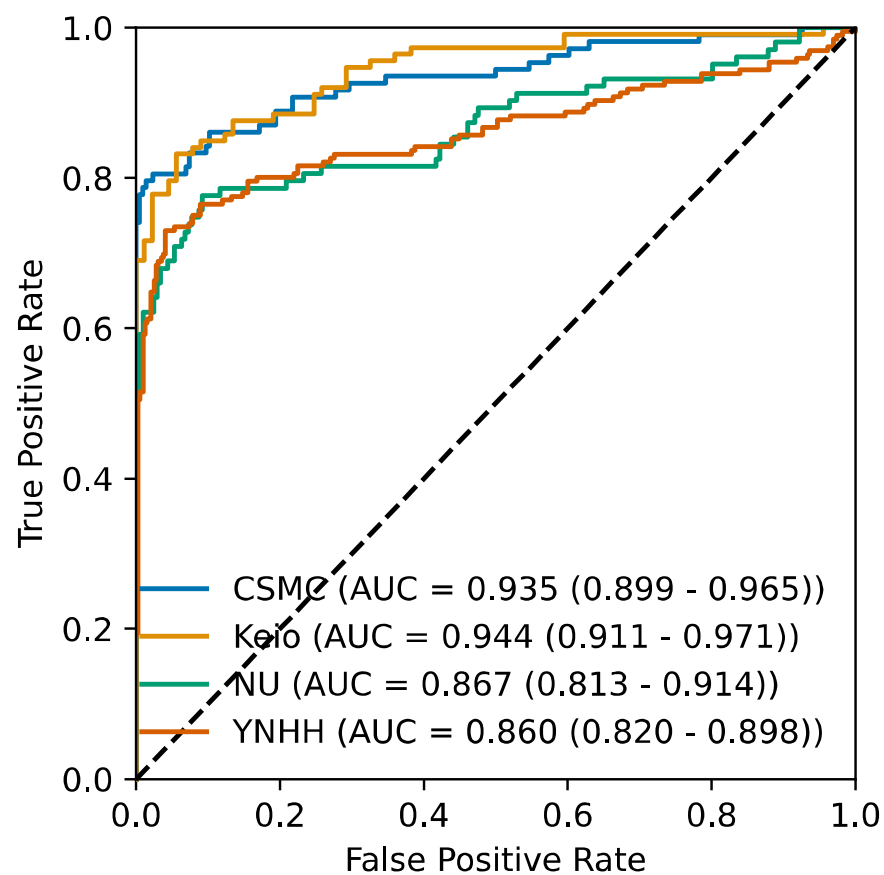
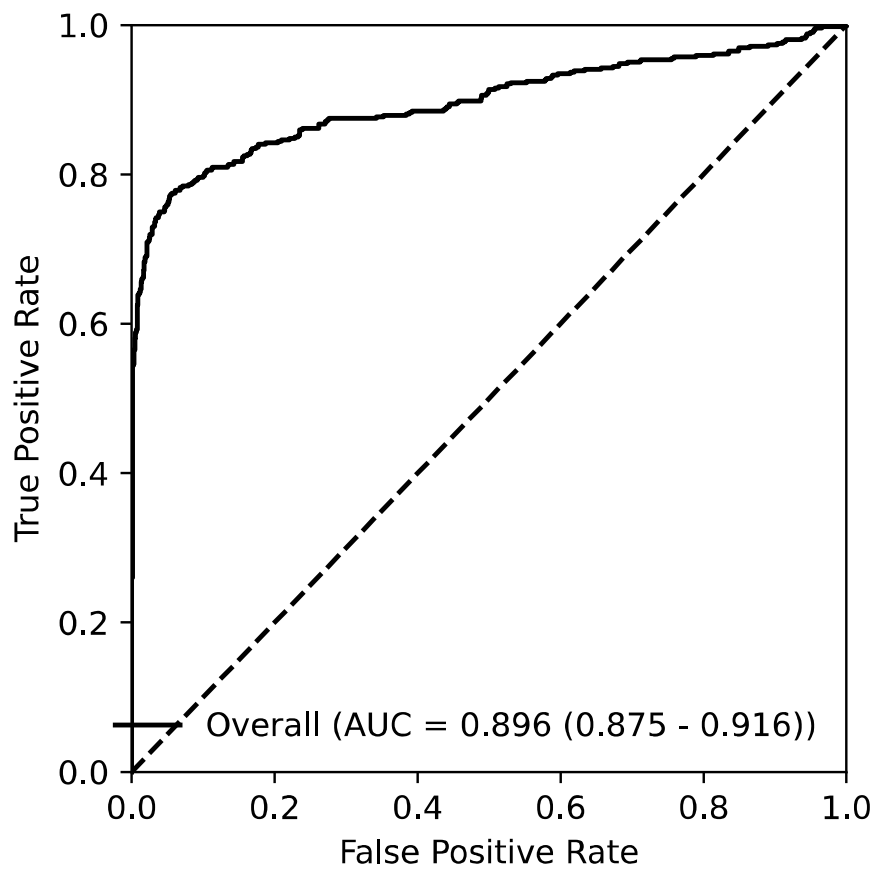
A few limitations are worth considering as further study is still warranted. Prospective trialing of CA screening approaches has not yet completed. There is less data on the true population prevalence of CA, which significantly impacts the PPV of any algorithm. Multiple other measurements and approaches have been suggested to screen for CA¹⁶, however our results is one of the few fully automated pipelines. Additionally, other work has assessed the performance of EchoNet-LVH in comparison to score-based decision aids and EHR-based algorithms and show EchoNet-LVH's superior performance³⁶. Furthermore, there is significant observer variability in most echocardiographic measurements³³, which limit the precision of approaches based on routine echo measurements alone¹⁸.

In this study comparing CA patients with patients who were referred for pyrophosphate scintigraphy but had CA ruled out, we demonstrate that IVSd/GLS can be used to identify CA in a population with high clinical suspicion for CA. This ratio has superior performance compared to individual echocardiographic measurements as well as other ratios that are already abnormal in patients at high suspicion for CA. If validated in future studies, incorporation of this easily obtainable measurement can assist with earlier diagnosis of CA resulting in reduced morbidity and mortality.

Disclosures

This work is funded by NIH NHLBI grants R00HL157421, R01HL173526, and R01HL173487 to DO, and a grant from Alexion AstraZeneca Rare Disease. GD is currently an employee of Meta. D.O. reports consulting fees and/or equity in Ultromics, InVision, EchoIQ, and Pfizer. National Heart, Lung, And Blood Institute of the National Institutes of Health (under award numbers R01HL167858 and K23HL153775 to R.K., and F32HL170592 to E.K.O.), National Institute on Aging of the National Institutes of Health (under award number R01AG089981 to R.K.), and the Doris Duke Charitable Foundation (under award number 2022060 to R.K.). FSA has received research support from Pfizer and Atman Health. All other authors declare no competing interests.

FIGURE 1. Receiver Operating Characteristic Curve for EchoNet-LVH



Overall performance of AI algorithm and subset by site. CSMC = Cedars-Sinai Medical Center, NU = Northwestern University, YNHH = Yale New Haven Hospital

TABLES

Participants	Median (IQR) or N (%)
Age	78 (72-84)
Men	1105 (77.7%)
Cardiac amyloidosis	231 (33.3%)
Subtype	
AL	118 (22.7%)
ATTR	386 (74.2%)
Other	16 (3.2%)
Age	
< 74	456 (32.0%)
75-84	626 (44.0%)
> 85	341(24.0%)
BMI	
< 25	604 (42.4%)
25-30	511 (35.9%)
> 30	308 (21.6%)
Ultrasound Manufacturer	
Philips	973 (68.4%)
GE	281 (19.7%)
Siemens	130 (9.1%)
Toshiba	39 (2.7%)

Table 1. Patient Characteristics

Group	n	Sensitivity (95% CI)	Specificity (95% CI)	PPV (95% CI)	NPV (95% CI)	AUROC (95% CI)
Overall	1423	0.644 (0.601 - 0.685)	0.988 (0.978 - 0.994)	0.968 (0.944 - 0.984)	0.828 (0.804 - 0.850)	0.896 (0.875 - 0.916)
CSMC	324	0.648 (0.550 - 0.738)	1.000 (0.983 - 1.000)	1.000 (0.949 - 1.000)	0.850 (0.800 - 0.892)	0.935 (0.899 - 0.965)
Keio	202	0.779 (0.691 - 0.851)	0.966 (0.905 - 0.993)	0.967 (0.907 - 0.993)	0.775 (0.686 - 0.849)	0.944 (0.911 - 0.971)
NU	309	0.621 (0.520 - 0.715)	0.981 (0.951 - 0.995)	0.941 (0.856 - 0.984)	0.838 (0.785 - 0.882)	0.867 (0.814 - 0.915)
YNHH	588	0.577 (0.504 - 0.647)	0.990 (0.974 - 0.997)	0.966 (0.915 - 0.991)	0.824 (0.786 - 0.857)	0.860 (0.818 - 0.898)

Table 2. Overall performance. CSMC = Cedars-Sinai Medical Center, NU = Northwestern University, YNHH = Yale New Haven Hospital, PPV = Positive Predictive Value, NPV = Negative Predictive Value

Group	n	Sensitivity (95% CI)	Specificity (95% CI)	PPV (95% CI)	NPV (95% CI)	AUROC (95% CI)
Sex						
Male	1105	0.655 (0.609 - 0.700)	0.987 (0.975 - 0.994)	0.970 (0.943 - 0.986)	0.813 (0.785 - 0.840)	0.893 (0.869 - 0.914)
Female	318	0.585 (0.471 - 0.693)	0.992 (0.970 - 0.999)	0.960 (0.863 - 0.995)	0.873 (0.827 - 0.911)	0.904 (0.849 - 0.950)
Race						
White	888	0.578 (0.515 - 0.639)	0.990 (0.979 - 0.996)	0.961 (0.918 - 0.986)	0.851 (0.823 - 0.876)	0.871 (0.837 - 0.902)
Asian	202	0.779 (0.691 - 0.851)	0.966 (0.905 - 0.993)	0.967 (0.907 - 0.993)	0.775 (0.686 - 0.849)	0.944 (0.911 - 0.971)
Black	174	0.642 (0.543 - 0.732)	0.985 (0.921 - 1.000)	0.986 (0.922 - 1.000)	0.638 (0.539 - 0.730)	0.884 (0.831 - 0.931)
Hispanic	66	0.688 (0.413 - 0.890)	1.000 (0.929 - 1.000)	1.000 (0.715 - 1.000)	0.909 (0.800 - 0.970)	0.963 (0.894 - 1.000)
Other	93	0.704 (0.498 - 0.862)	0.985 (0.918 - 1.000)	0.950 (0.751 - 0.999)	0.890 (0.795 - 0.951)	0.880 (0.762 - 0.973)
Age						
65 - 74	434	0.646 (0.568 - 0.719)	0.989 (0.968 - 0.998)	0.972 (0.922 - 0.994)	0.822 (0.775 - 0.862)	0.918 (0.886 - 0.946)
75 - 84	626	0.629 (0.563 - 0.692)	0.985 (0.967 - 0.994)	0.960 (0.915 - 0.985)	0.821 (0.784 - 0.855)	0.874 (0.837 - 0.908)
85+	341	0.643 (0.549 - 0.731)	0.991 (0.968 - 0.999)	0.974 (0.908 - 0.997)	0.845 (0.796 - 0.887)	0.903 (0.860 - 0.941)
BMI						
<25	604	0.656 (0.595 - 0.714)	0.980 (0.959 - 0.992)	0.960 (0.919 - 0.984)	0.795 (0.754 - 0.832)	0.886 (0.854 - 0.915)
25 - 30	511	0.655 (0.583 - 0.721)	0.987 (0.968 - 0.997)	0.969 (0.924 - 0.992)	0.824 (0.782 - 0.861)	0.906 (0.873 - 0.935)
>30	308	0.571 (0.447 - 0.689)	1.000 (0.985 - 1.000)	1.000 (0.912 - 1.000)	0.888 (0.844 - 0.923)	0.880 (0.812 - 0.938)
Amyloid subtype						

AL	1021	0.661 (0.568 - 0.746)	0.988 (0.978 - 0.994)	0.876 (0.790 - 0.937)	0.957 (0.942 - 0.969)	0.921 (0.882 - 0.955)
ATTR	1289	0.640 (0.590 - 0.688)	0.988 (0.978 - 0.994)	0.957 (0.925 - 0.979)	0.865 (0.843 - 0.885)	0.887 (0.862 - 0.911)
Other	919	0.625 (0.354 - 0.848)	0.988 (0.978 - 0.994)	0.476 (0.257 - 0.702)	0.993 (0.986 - 0.998)	0.935 (0.866 - 0.994)
Ultrasound Manufacturer						
Philips	973	0.594 (0.540 - 0.645)	0.992 (0.981 - 0.997)	0.977 (0.946 - 0.992)	0.812 (0.782 - 0.839)	0.889 (0.862 - 0.914)
GE Ultrasound	187	0.741 (0.610 - 0.847)	0.977 (0.934 - 0.995)	0.935 (0.821 - 0.986)	0.894 (0.831 - 0.939)	0.860 (0.782 - 0.931)
Siemens	130	0.714 (0.554 - 0.843)	0.989 (0.938 - 1.000)	0.968 (0.833 - 0.999)	0.879 (0.798 - 0.936)	0.942 (0.888 - 0.984)
GE Vingmed	94	0.787 (0.643 - 0.893)	0.957 (0.855 - 0.995)	0.949 (0.827 - 0.994)	0.818 (0.691 - 0.909)	0.942 (0.891 - 0.980)
TOSHIBA	39	0.762 (0.528 - 0.918)	1.000 (0.815 - 1.000)	1.000 (0.794 - 1.000)	0.783 (0.563 - 0.925)	0.931 (0.824 - 1.000)

Table 3. Subgroup performance. PPV = Positive Predictive Value, NPV = Negative Predictive Value, BMI = Body Mass Index

REFERENCES

1. Schirmer H, Lunde P, Rasmussen K. Prevalence of left ventricular hypertrophy in a general population; The Tromso Study. *Eur Heart J*. 1999;20(6):429-438.
2. Kittleson MM, Ruberg FL, Ambardekar AV, et al. 2023 ACC Expert Consensus Decision Pathway on Comprehensive Multidisciplinary Care for the Patient With Cardiac Amyloidosis: A Report of the American College of Cardiology Solution Set Oversight Committee. *J Am Coll Cardiol*. 2023;81(11):1076-1126.
3. Tanskanen M, Peuralinna T, Polvikoski T, et al. Senile systemic amyloidosis affects 25% of the very aged and associates with genetic variation in alpha2-macroglobulin and tau: a population-based autopsy study. *Ann Med*. 2008;40(3):232-239.
4. Gonzalez-Lopez E, Gallego-Delgado M, Guzzo-Merello G, et al. Wild-type transthyretin amyloidosis as a cause of heart failure with preserved ejection fraction. *Eur Heart J*. 2015;36(38):2585-2594.
5. Nitsche C, Scully PR, Patel KP, et al. Prevalence and Outcomes of Concomitant Aortic Stenosis and Cardiac Amyloidosis. *J Am Coll Cardiol*. 2021;77(2):128-139.
6. Kastiris E, Palladini G, Minnema MC, et al. Daratumumab-Based Treatment for Immunoglobulin Light-Chain Amyloidosis. *N Engl J Med*. 2021;385(1):46-58.
7. Maurer MS, Schwartz JH, Gundapaneni B, et al. Tafamidis Treatment for Patients with Transthyretin Amyloid Cardiomyopathy. *N Engl J Med*. 2018;379(11):1007-1016.
8. Ruberg FL, Grogan M, Hanna M, Kelly JW, Maurer MS. Transthyretin Amyloid Cardiomyopathy: JACC State-of-the-Art Review. *J Am Coll Cardiol*. 2019;73(22):2872-2891.
9. Falk RH, Alexander KM, Liao R, Dorbala S. AL (Light-Chain) Cardiac Amyloidosis: A Review of Diagnosis and Therapy. *J Am Coll Cardiol*. 2016;68(12):1323-1341.
10. Mohty D, Damy T, Cosnay P, et al. Cardiac amyloidosis: updates in diagnosis and management. *Arch Cardiovasc Dis*. 2013;106(10):528-540.
11. Weidemann F, Niemann M, Ertl G, Stork S. The different faces of echocardiographic left ventricular hypertrophy: clues to the etiology. *J Am Soc Echocardiogr*. 2010;23(8):793-801.
12. Cuddy SAM, Chetrit M, Jankowski M, et al. Practical Points for Echocardiography in Cardiac Amyloidosis. *J Am Soc Echocardiogr*. 2022;35(9):A31-A40.
13. Cyrille NB, Goldsmith J, Alvarez J, Maurer MS. Prevalence and prognostic significance of low QRS voltage among the three main types of cardiac amyloidosis. *Am J Cardiol*. 2014;114(7):1089-1093.
14. Potter E, Marwick TH. Assessment of Left Ventricular Function by Echocardiography: The Case for Routinely Adding Global Longitudinal Strain to Ejection Fraction. *JACC Cardiovasc Imaging*. 2018;11(2 Pt 1):260-274.
15. Karlsen S, Dahlslett T, Grenne B, et al. Global longitudinal strain is a more reproducible measure of left ventricular function than ejection fraction regardless of echocardiographic training. *Cardiovasc Ultrasound*. 2019;17(1):18.
16. Phelan D, Collier P, Thavendiranathan P, et al. Relative apical sparing of longitudinal strain using two-dimensional speckle-tracking echocardiography is both sensitive and specific for the diagnosis of cardiac amyloidosis. *Heart*. 2012;98(19):1442-1448.
17. Cotella J, Randazzo M, Maurer MS, et al. Limitations of Apical Sparing Pattern in Cardiac Amyloidosis: A Multicenter Echocardiographic Study. *Eur Heart J Cardiovasc Imaging*. 2024.
18. Pagourelis ED, Mirea O, Duchenne J, et al. Echo Parameters for Differential Diagnosis in Cardiac Amyloidosis: A Head-to-Head Comparison of Deformation and Nondeformation Parameters. *Circ Cardiovasc Imaging*. 2017;10(3):e005588.

19. Ferkh A, Tjahjadi C, Stefani L, et al. Cardiac "hypertrophy" phenotyping: differentiating aetiologies with increased left ventricular wall thickness on echocardiography. *Front Cardiovasc Med.* 2023;10:1183485.
20. Duffy G, Cheng PP, Yuan N. et al. High-throughput precision phenotyping of left ventricular hypertrophy with cardiovascular deep learning. *JAMA Cardiology.* 2022. 7(4):386-395
21. Rubin J, Maurer MS. Cardiac Amyloidosis: Overlooked, Underappreciated, and Treatable. *Annu Rev Med.* 2020;71:203-219.
22. Ichimata S, Hata Y, Hirono K, Yamaguchi Y, Nishida N. Clinicopathological features of clinically undiagnosed sporadic transthyretin cardiac amyloidosis: a forensic autopsy-based series. *Amyloid.* 2021;28(2):125-133.
23. Rahman JE, Helou EF, Gelzer-Bell R, et al. Noninvasive diagnosis of biopsy-proven cardiac amyloidosis. *J Am Coll Cardiol.* 2004;43(3):410-415.
24. Gertz MA, Comenzo R, Falk RH, et al. Definition of organ involvement and treatment response in immunoglobulin light chain amyloidosis (AL): a consensus opinion from the 10th International Symposium on Amyloid and Amyloidosis, Tours, France, 18-22 April 2004. *Am J Hematol.* 2005;79(4):319-328.
25. Suresh R, Grogan M, Maleszewski JJ, et al. Advanced cardiac amyloidosis associated with normal interventricular septal thickness: an uncommon presentation of infiltrative cardiomyopathy. *J Am Soc Echocardiogr.* 2014;27(4):440-447.
26. Tanaka H. Efficacy of echocardiography for differential diagnosis of left ventricular hypertrophy: special focus on speckle-tracking longitudinal strain. *J Echocardiogr.* 2021;19(2):71-79.
27. Maron BJ, Desai MY, Nishimura RA, et al. Diagnosis and Evaluation of Hypertrophic Cardiomyopathy: JACC State-of-the-Art Review. *J Am Coll Cardiol.* 2022;79(4):372-389.
28. Kyrouac D, Schiffer W, Lennep B, et al. Echocardiographic and clinical predictors of cardiac amyloidosis: limitations of apical sparing. *ESC Heart Fail.* 2022;9(1):385-397.
29. Redfield MM, Borlaug BA. Heart Failure With Preserved Ejection Fraction: A Review. *JAMA.* 2023;329(10):827-838.
30. Rader F, Sachdev E, Arsanjani R, Siegel RJ. Left ventricular hypertrophy in valvular aortic stenosis: mechanisms and clinical implications. *Am J Med.* 2015;128(4):344-352.
31. Miller P, Maurer MS, Einstein AJ, Elias P, Poterucha TJ. Recognizing Cardiac Amyloidosis Phenotype by Echocardiography Increases Downstream Testing. *J Am Soc Echocardiogr.* 2023;36(12):1326-1329.
32. Boldrini M, Cappelli F, Chacko L, et al. Multiparametric Echocardiography Scores for the Diagnosis of Cardiac Amyloidosis. *JACC Cardiovasc Imaging.* 2020;13(4):909-920.
33. Farsalinos KE, Daraban AM, Unlu S, Thomas JD, Badano LP, Voigt JU. Head-to-Head Comparison of Global Longitudinal Strain Measurements among Nine Different Vendors: The EACVI/ASE Inter-Vendor Comparison Study. *J Am Soc Echocardiogr.* 2015;28(10):1171-1181, e1172.
34. Tokai T, Takashio S, Kawano Y, et al. Assessing the treatment effect of daratumumab by serial measurements of cardiac biomarkers and imaging parameters in light-chain cardiac amyloidosis. *J Cardiol Cases.* 2022;26(4):301-304.
35. Giblin GT, Cuddy SAM, Gonzalez-Lopez E, et al. Effect of tafamidis on global longitudinal strain and myocardial work in transthyretin cardiac amyloidosis. *Eur Heart J Cardiovasc Imaging.* 2022;23(8):1029-1039.
36. S Jonathan Hourmozdi, Nicholas Easton, Simon Benigeri, James D Thomas, Akhil Narang, David Ouyang, Grant Duffy, Ike Okwuosa, Adrienne Kline, Abel N Kho, Yuan Luo, Sanjiv J Shah, Faraz S Ahmad. Evaluating the performance and potential bias of predicting models for the detection of transthyretin cardiac amyloidosis, *medRxiv.* (2024).

It is made available under a [CC-BY 4.0 International license](#) .